

# Characterisation of thermal barrier coatings and ultra high temperature composites deposited in a low pressure plasma reactor

C. Fourmond<sup>a</sup>, G. Da Rold<sup>a</sup>, F. Rousseau<sup>b,\*</sup>, C. Guyon<sup>b</sup>, S. Cavadias<sup>a</sup>, D. Morvan<sup>b</sup>, R. Mévrel<sup>c</sup>

<sup>a</sup> UPMC, Plasma Process Engineering and Surface Treatment Laboratory, 11 rue Pierre et Marie Curie, 75005 Paris, France

<sup>b</sup> Ecole Nationale Supérieure de Chimie de Paris – ParisTech, Plasma Process Engineering and Surface Treatment Laboratory, 11 rue Pierre et Marie Curie, 75005 Paris, France

<sup>c</sup> ONERA, DMSM, 29 avenue de la division Leclerc, 92322 Chatillon, Cedex, France

Received 13 December 2010; received in revised form 31 May 2011; accepted 8 June 2011

Available online 2 July 2011

## Abstract

A low pressure plasma process working at 600–800 Pa was used to deposit from aqueous solution ZrO<sub>2</sub>–4 mol% Y<sub>2</sub>O<sub>3</sub> (Ytria partially stabilized Zirconia–YpSZ) layers and stacks of Ta<sub>2</sub>O<sub>5</sub>/YpSZ layers for use as thermal barrier coatings (TBC). The observation of the cross section revealed a high porosity. The thermal diffusivity of the layers ( $1 \times 10^{-7} \text{ m}^2 \text{ s}^{-1}$ ) was measured by a laser flash technique and compared with values obtained on air plasma sprayed material ( $3 \times 10^{-7} \text{ m}^2 \text{ s}^{-1}$ ). The plasma reactor were also used to deposit ZrB<sub>2</sub>–ZrO<sub>2</sub>–SiC layers used as Ultra High Temperature Composite (UHTC) from aqueous solutions of zirconyl and Boron nitrates containing suspensions of SiC. Layers up to 100 μm thick were obtained on SiC substrates. XRD was used to study the crystallinity of the layer. The presence of ZrB<sub>2</sub> and SiC phases was confirmed after the deposition. XRD analysis showed that heat treatment at 1073 K under oxidizing conditions led to the loss of ZrB<sub>2</sub> and the appearance of ZrO<sub>2</sub> phases. To understand the behaviour of the layers to interaction with atomic oxygen (combustion for TBC and spacecraft re-entry phase for UHTC), we have measured the atomic oxygen recombination coefficient to determine the number of adsorption sites on the surface of the coatings. This was accomplished by using a low pressure plasma reactor coupled with optical spectroscopic measurements as a diagnostic technique.

© 2011 Elsevier Ltd. All rights reserved.

**Keywords:** Traditional ceramics; Composites; Nanocomposites; Porosity; Thermal properties

## 1. Introduction

Research to reduce the consumption of fuel and the emissions of pollutants by turbines is a current subject of interest in aeronautics. For example, increasing the temperature of combustion leads to more efficient conversion of fuel into energy. The lifetime of materials used in turbines need to be increased by augmenting their resistance to corrosion phenomena at high temperature. Such improvements can also decrease the cost of turbines. One of the solutions consists in covering the combustion chamber and the blades with a thermal barrier coating (TBC). A TBC is a thick oxide layer used to protect the alloy of the blades and the combustion chamber against high temperatures. The oxide generally used is zirconia partially stabilized with yttrium (YpSZ).<sup>1</sup> This oxide has a low thermal diffusivity

(2.5 W/m K with 1273 K as well as a good coefficient of thermal expansion ( $\sim 10^{-5}/^\circ\text{C}$ ).<sup>2</sup> These characteristics naturally make it a good material for use as a TBC. Several deposition techniques are used to obtain YpSZ layers such as EBPVD,<sup>3</sup> but also APS,<sup>4</sup> sol–gel,<sup>5</sup> PECVD,<sup>6</sup> and SPS<sup>7</sup>... In all cases, the YpSZ TBC should be highly porous in order to decrease the thermal diffusivity of the layers. For example, the SPS technique permits the deposition of 20% porous YpSZ. Covering YpSZ by Ta<sub>2</sub>O<sub>5</sub> is envisaged to increase the lifetime of the TBC.<sup>8</sup> The tantalum oxide, porous or not, can act as a protective layer against the chemical attack of CaO–MgO–Al<sub>2</sub>O<sub>3</sub>–SiO<sub>2</sub> dusts which are present in the combustion chamber.<sup>9</sup> B.A. Nagaraj<sup>8</sup> has reported that a tantalum oxide deposited by EBPVD or Plasma Spray onto the thermal barrier coating has dielectric properties such that the CMAS deposits are less able to adhere to the exposed surface of the outer layer. As a result, the CMAS are unable to infiltrate the porous surface structure of the thermal barrier coating, and thus cannot attack and destroy YpSZ.

\* Corresponding author. Tel.: +33 144276825.

E-mail address: [frederic-rousseau@chimie-paristech.fr](mailto:frederic-rousseau@chimie-paristech.fr) (F. Rousseau).

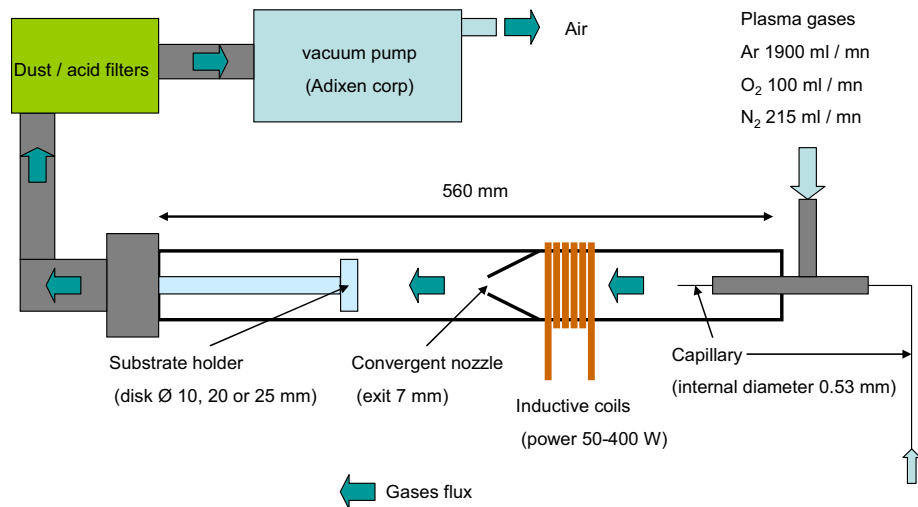


Fig. 1. Description of the low pressure plasma process developed to deposit thick  $\text{ZrB}_2\text{-ZrO}_2\text{-SiC}$  coatings.

High temperature composite layers are also investigated for aerospace applications, especially for the protection of re-entry vehicles against high temperature during re-entry into the earth's atmosphere. Due to the high temperature created by the interaction between vehicle and the atmosphere ( $T > 1773$  K), UHTC materials (Ultra High-Temperature Composite) are now being studied.<sup>10–13</sup> For example,  $\text{ZrB}_2$  presents a unique combination of mechanical and physical properties, including a high melting point ( $>3273$  K), high thermal and electric conductivity, chemical inertia which counters molten metals, and very great impact resistance.<sup>14</sup> These characteristics of  $\text{ZrB}_2$  make it an excellent candidate for a standard UHTC material. However, it may be very difficult to synthesize this kind of material as a thick layer with strong adhesion to the substrate.

In this work, a deposition technique developed in Chimie ParisTech was studied to deposit both YpSZ layers for TBC applications and  $\text{ZrB}_2\text{-ZrO}_2\text{-SiC}$  coatings to be used as UHTC materials. The principle of the deposition technique consists of introducing an aqueous solution of a nitrate salt or a solid suspension in water into a low pressure plasma discharge.<sup>15–17</sup> The aim of this work was to study the possibility of obtaining thick ceramic coatings using a plasma power of less than 0.5 kW. This power value was less than one tenth of that used for the "usual" deposition techniques such as Solution Plasma Spray and EBPVD (Power  $> 10$  kW).<sup>3,7</sup> After the deposition, coatings were annealed and analyzed by several techniques (SEM, XRD, Laser Flash Technique, catalicity measurements) to study the stability, the morphology, the properties and the resistance of the deposited material.

## 2. Description of the low pressure plasma process and analyses performed on the oxide coatings

### 2.1. Principle of the plasma process

The deposition process consists of using the oxidizing properties of an Ar/Oxygen discharge to transform precursor nitrate

salts into oxide layers. For example, a  $\text{ZrO}_2$  coating can be obtained on a substrate when an aqueous solution containing zirconyl nitrates is injected into the plasma reactor. The plasma reactor consisted of a pyrex tube equipped with a convergent nozzle (pressure: 600–800 Pa). The injection system used for the deposition of YpSZ and  $\text{Ta}_2\text{O}_5$  was described previously and additional information can be found in the literature.<sup>17</sup> Another injection system was developed for the deposition of  $\text{ZrB}_2\text{-ZrO}_2\text{-SiC}$  from an aqueous solution containing a SiC suspension. All the characteristics of the deposition technique are summarized in Fig. 1.

The chemical reactions which occur in the discharge lead to the formation of oxidant species such as O (from  $\text{O}_2$ ) and  $\text{OH}^\bullet$  (from the water of the aqueous solution) which are favorable reagents to transform precursor nitrate salts into oxide layers. One of the advantages of inductive plasma is the purity of the products which is high because the discharge is generated without internal electrodes which could otherwise pollute due to consumption and corrosion.

The coating deposition consisted of two steps. The synthesis of YpSZ was described previously.<sup>17</sup> For the deposition of  $\text{ZrB}_2\text{-ZrO}_2\text{-SiC}$ , the aqueous solution was injected during 1 min into a 120 W plasma discharge by means of a capillary as shown in Fig. 1 (step 1). As the liquid exits the capillary, the formation of aerosol occurs and the nitrate salt reacted with the oxidant species of the plasma to form a deposit on a substrate. The second step consisted of a 10 min post treatment using a 180 W plasma discharge, in which only air flowed through the capillary. The oxidant reagents present in the plasma discharge then eliminated residual water from the deposit and finished the transformation of the nitrates into the oxide layer. The cycle was repeated until the desired thickness of oxide was obtained. It is essential to note that the temperature of the substrate during the post treatment is less than 573 K. After the synthesis, a heat treatment was performed on the oxides to complete the elimination of nitrate and water and to crystallize the layers. This heat treatment was performed as follows: 1273 K for 4 h in air (heating and cooling rate:  $473 \text{ K h}^{-1}$ ).

## 2.2. Aqueous solution used for the deposition of coatings

### 2.2.1. $ZrO_2$ – $Y_2O_3$ and $ZrO_2$ – $Y_2O_3$ / $Ta_2O_5$

The precursors used for the deposition of YpSZ on 25 mm alumina disk consisted of a mixture of ZrO and Y nitrate powders dissolved in water in order to obtain YpSZ containing 5.26 mol%  $Y_2O_3$ . The characteristics of the nitrates are following:

- Zirconyl nitrates Acros Organics 99.5%:  $[ZrO(NO_3)_2] = 0.34 \text{ mol L}^{-1}$ ,
- Yttrium nitrates Acros Organics 99.9%:  $[Y(NO_3)_3] = 0.04 \text{ mol L}^{-1}$ .

The solution containing Tantalum used to obtain  $Ta_2O_5$  was home made at ONERA. The composition of the solution of Tantalum was  $10 \text{ g L}^{-1}$  of Ta,  $40 \text{ g L}^{-1}$   $H_2C_2O_4$  and 0.4%  $H_2SO_4$ . Concerning the deposition of YpSZ/ $Ta_2O_5$  layer stacks, an aqueous solution containing ZrO and Y nitrates was first injected into the reactor. When the YpSZ coating was thick enough, the solution of Ta was introduced in order for it to then be covered by a thin layer of  $Ta_2O_5$ .

### 2.2.2. $ZrB_2$ – $ZrO_2$ – $SiC$

The aqueous solution was prepared in order to obtain a 20 vol%  $ZrB_2$ – $SiC$  on a 25 mm  $SiC$  disk. The characteristics of the precursors used to prepare the solution are summed up here:

- Zirconyl nitrate Acros Organics 99.5%,
- Boron solution used for the calibration of ICP (Sigma–Aldrich), 10,034 ppm of B in water, 0.1%  $NH_4OH$ ,
- $SiC$  powder,  $\beta$  phase,  $\rho = 3.217 \text{ g cm}^{-3}$ , Alfa Aesar.

The aqueous solution obtained from the mixture of precursors contained a very high concentration of suspended  $SiC$  and exhibited a high viscosity.

## 2.3. Analyses used to study the morphology, structure and properties

Scanning Electron Microscopy (SEM) was used to study the morphology of the coatings. The observation of the cross section revealed the porosity and the attachment of the coatings to the substrate. X-ray diffraction (XRD) was employed to study the crystallinity, purity, thermal stability and the composition of the deposited coatings. For the case of the YpSZ layer, the thermal diffusivity was measured by a  $CO_2$  laser technique as a function of the temperature.<sup>18,19</sup> The thermal diffusivity was compared to values acquired on two other YpSZ samples synthesized by other techniques. The aim was to determine if the TBC obtained in the low pressure plasma process was of the same quality as those deposited by an industrial plasma technique (APS).<sup>19</sup>

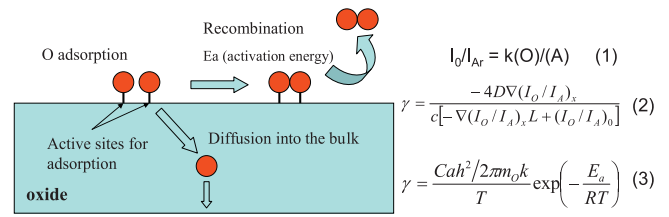


Fig. 2. Reactivity of oxide with atomic oxygen (recombination/diffusion) and equation used to determine the number of active sites and the  $\gamma$  coefficient for the recombination of  $O_2$ .

## 2.4. Properties of the surface: measure of the recombination of oxygen

The surface of the oxide layers used as TBC in aeronautics and as UHTC in aerospace are in contact with O at high temperature. The atomic oxygen results from the dissociation of  $O_2$  due to the high temperatures in the combustion in a turbine or is produced in the plasma surrounding a spacecraft during re-entry in the atmosphere. It is important to investigate the recombination of atomic oxygen on the surface of the coating. By considering  $Ta_2O_5$ , which is envisaged to function as a protective layer against CMAS attack, the aim of the analysis was to determine if the interaction with O was similar to that observed for YpSZ. Concerning the  $ZrB_2$ – $ZrO_2$ – $SiC$  coating, the objectives of such analyses was to compare with the  $SiC$  material usually employed to protect the space shuttle.

The samples were placed in a low pressure plasma reactor which produces atomic oxygen.<sup>20–22</sup> As shown in Fig. 2, the number of adsorbed O depends on the number of active sites. It can be supposed that the atomic oxygen is eliminated from the surface by two possible pathways:

- Recombination to form  $O_2$  (depends on the number of active recombination sites: Ca),
- Diffusion into the bulk (favored if  $\gamma$  are low) or the oxidation of the coating if it is not yet complete.

The recombination coefficient was calculated using the actinometry spectroscopic method. O atom concentration had been monitored with optical emissions from O (844.6 nm) and Ar (811.5 nm). The ratio  $I_O/I_{Ar}$  was proportional to the concentration ratio of O and Ar according to the following relation:

$$\frac{I_O}{I_{Ar}} \propto \frac{(O)}{(Ar)} \quad (1)$$

The movement of oxygen atoms in the boundary layer near the sample was controlled by diffusion and described by the general diffusion equation. The recombination coefficient  $\gamma$  was calculated from the atomic oxygen concentration profile along the reactor by using Eq. (2):

$$\gamma = \frac{-4D\nabla(I_O/I_A)_x}{c[-\nabla(I_O/I_A)_x L + (I_O/I_A)_0]} \quad (2)$$

where  $D$  is the binary coefficient ( $m^2 s^{-1}$ ),  $c$  the atomic velocity ( $m s^{-1}$ ),  $L$  the width of the boundary layer ( $m$ ),  $\nabla(I_O/I_{Ar})_x$

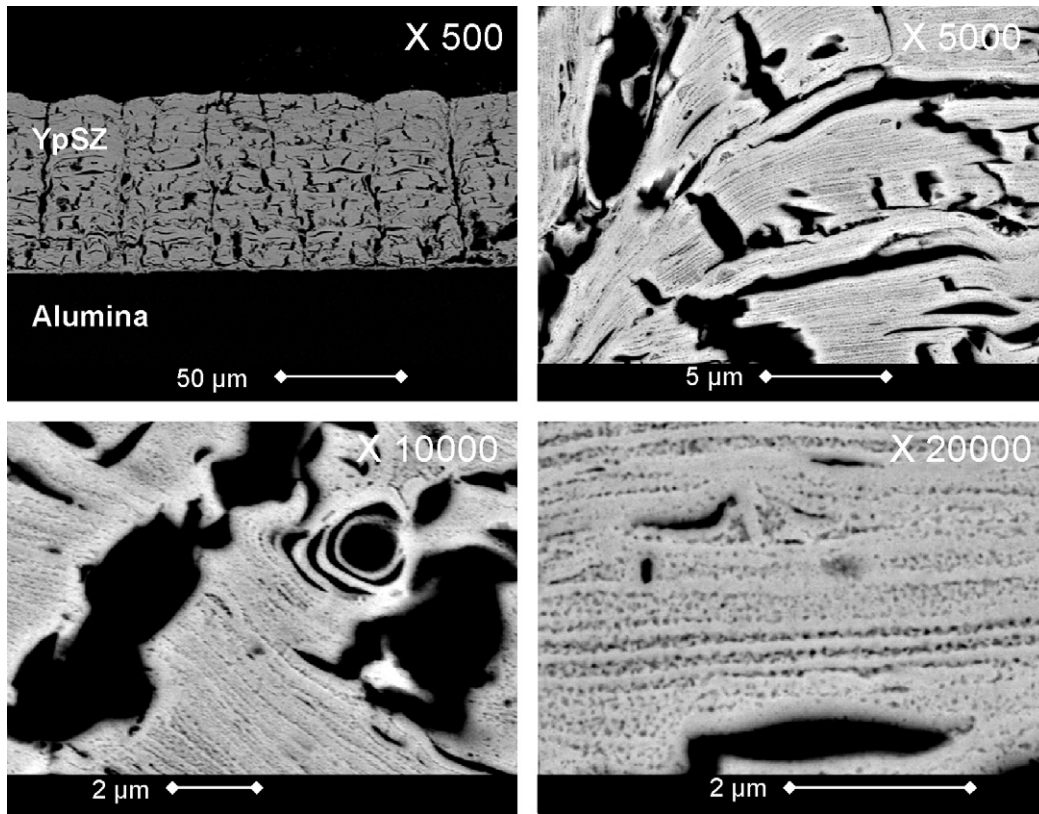


Fig. 3. Cross section of YpSZ layer deposited on alumina and heat-treated at 1273 K for 4 h.

the axial concentration gradient and  $(I_O/I_{Ar})_0$  the steady state concentration.

The recombination coefficient is a function of the surface temperature according to the following Eq. (3):

$$\gamma = \frac{C_a h^2 / 2\pi m_O k}{T} \exp\left(-\frac{E_a}{RT}\right) \quad (3)$$

where  $C_a$  is the number of active sites ( $\text{atoms m}^{-2}$ ),  $h$  the Planck constant ( $6.626 \times 10^{-34} \text{ J s}$ ),  $m_O$  mass of an oxygen atom (kg),  $k$  the Boltzmann constant ( $1.38065 \times 10^{-23} \text{ J K}^{-1}$ ),  $T$  the temperature in K,  $E_a$  is the activation energy of the surface reaction ( $\text{J mol}^{-1}$ ) and  $R$  the gas constant ( $8.314 \text{ J mol}^{-1} \text{ K}^{-1}$ ). The activation energy of the process and the number of active sites could be deduced by calculating  $\gamma$  with Eq. (2) and by plotting  $\ln(\gamma T)$ .<sup>2</sup>

### 3. Characteristics of YpSZ and YpSZ/Ta<sub>2</sub>O<sub>5</sub> coatings

#### 3.1. YpSZ layers deposited on alumina substrate

The observation of the cross section of YpSZ after the heat treatment revealed a thick porous coating up to  $80 \mu\text{m}$  thick as shown in Fig. 3. By considering the time needed for the deposition of YpSZ (injection and post treatment), the growth rate was calculated to be around  $10 \mu\text{m h}^{-1}$ . It can be seen that the YpSZ/alumina interface is typical of a coating adhering strongly on the substrate. Cracks are present between pores in the cross section and some of them seem to extend from the surface all the way down to the alumina substrate. These cracks are a favorable

feature to increase the thermo-mechanical resistance of the YSZ coating. The SEM shows that the YpSZ layer exhibits pores with micrometric and nanometric sizes. By considering only the micrometric pores, and by using software called Visilog, the porosity was estimated to be around 25% (similar to SPS technique<sup>7</sup>). Water porosimetry was performed to measure the total porosity of the YpSZ coating. The total porosity was found to be 50% and the density was  $3.1 \text{ g cm}^{-3}$ . It is the presence of many nanometric pores which permits the coating to be highly porous. By observing the nano-pores under higher magnification, it can be seen in Fig. 3 that their size is less than 100 nm. The nano-porosity exhibits a horizontal lamellar nano-structure as shown at high magnification ( $\times 20,000$ ). Such nano-structure could be a favorable feature to decrease the thermal diffusivity of the TBC.

The thermal diffusivity of the YpSZ coating was measured using a laser CO<sub>2</sub> flash technique. The results are summarized in Fig. 4. The highest diffusivity values were obtained from a single crystal, that is for a dense material.<sup>18</sup> The curves with intermediate values are typical of air plasma sprayed materials.<sup>19</sup> The curve exhibiting lower values corresponds to the YpSZ coating deposited in the low pressure plasma process after a heat treatment of 2 h at 1273 K. The results are in accordance with the SEM observation. The nano porosity probably leads to a decrease of the thermal diffusivity values. The voids and the lamellar nano structure contribute to a decrease in the heat flow that goes from the surface to the substrate. Further work will consist of the study of the thermal stability of the nano pores at high temperature (more than 1373 K) and the measurement



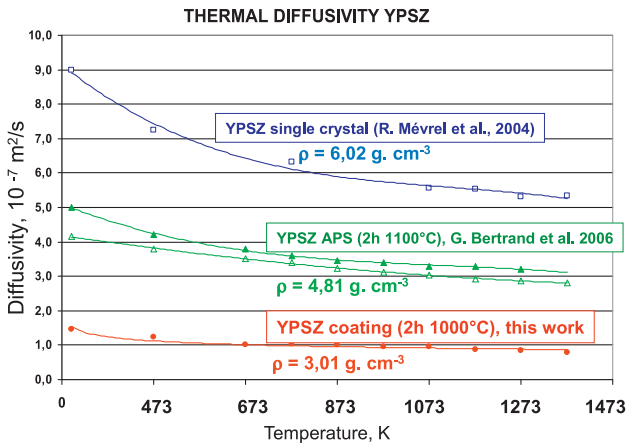


Fig. 4. Thermal diffusivity of YpSZ measured as a function of the temperature by a laser CO<sub>2</sub> flash technique.<sup>18,19</sup>

of the thermal conductivity of YpSZ in order to compare with classical techniques such as EBPVD and SPS.

### 3.2. Deposition of YpSZ/Ta<sub>2</sub>O<sub>5</sub> stack

Fig. 5 presents the cross section of a stack of thin YpSZ/Ta<sub>2</sub>O<sub>5</sub> layers observed by SEM. As expected, the nano pores previously described can be seen in the YpSZ layers. It can be observed that porous Ta<sub>2</sub>O<sub>5</sub> fully covers the surface of YpSZ. EDX analyses performed on the cross section of the stack confirmed the presence of Ta on the partially stabilized zirconia. No Tantalum was detected in the YpSZ coating.

### 3.3. Recombination of oxygen at the surface of YpSZ and Ta<sub>2</sub>O<sub>5</sub>

In a turbine, the TBC is deposited onto a bondcoat layer, which permits the YpSZ coating to adhere to the super-alloyed blade. It is well-known that YpSZ contributes to the formation of a thin alumina coating (thermally grown oxide–TGO) between the TBC and the boundary layer due to the dissociation and the diffusion of O into the zirconia at high temperature. An alumina coating which is too thick leads to the delamination and destruction of the TBC. Covering YpSZ by Ta<sub>2</sub>O<sub>5</sub> could be a favorable feature to protect the TBC against CMAS, but it could also increase the dissociation and the diffusion of oxygen to the

zirconia/boundary interface. The objective is then to determine if the reactivity of YpSZ and Ta<sub>2</sub>O<sub>5</sub> with oxygen atom is the same by measuring the recombination of O<sub>2</sub> at the surface.

Fig. 6 shows the evolution of the recombination coefficient as a function of the surface temperature measured on the alumina substrate, YpSZ and Tantalum oxide. By comparing the three different samples, it can be observed that the recombination coefficient increases with the temperature, but that the Ta<sub>2</sub>O<sub>5</sub> exhibits the higher  $\gamma$  coefficient at 1073 K. The analyses show that the coatings exhibit different surface properties upon reaction with oxygen. The surface of Ta<sub>2</sub>O<sub>5</sub> exhibits a lower number of active sites than YpSZ which is a favorable feature to limit the adsorption of O. At the same time the recombination of O<sub>2</sub> is higher for the tantalum oxide. It could be supposed that the small quantity of adsorbed O is eliminated under O<sub>2</sub> instead of diffusing into the bulk of the material. Currently, it is not possible to definitively determine whether the Tantalum oxide is able to increase or decrease the diffusion of oxygen into the bulk and additional studies must be done. Further work will consist of coupling measurement of the  $\gamma$  coefficient using labeled O<sup>18</sup> oxygen as the working gas with SIMS analyses to understand the mechanism for the diffusion of oxygen into YpSZ and Tantalum oxide. Employing Ta<sub>2</sub>O<sub>5</sub> as a protective coating and as a diffusion barrier would be interesting to improve the lifetime of the TBC.

## 4. Characteristics of ZrB<sub>2</sub>–ZrO<sub>2</sub>–SiC coatings

### 4.1. Deposition of ZrB<sub>2</sub>–ZrO<sub>2</sub>–SiC coatings

A 100  $\mu\text{m}$  thick ZrB<sub>2</sub>–ZrO<sub>2</sub>–SiC coating was obtained by using the low pressure plasma reactor (growth rate 60  $\mu\text{m h}^{-1}$ ). The variation of the composition of the layer was studied by X-ray diffraction analysis (Fig. 7), both after a simple heat treatment (1273 K–4 h) and after heat treatment coupled to oxidation by plasma exposure during the measurements of the recombination coefficient (1073 K during 2 min). The indexation of the peaks was performed using values found in the literature.<sup>23</sup> In the first case, peaks of high intensity were found for silicon carbide and ZrB<sub>2</sub>. In the second case, the oxidation due to the air plasma treatment under thermal condition (1073 K) changed the deposited layer into a ZrB<sub>2</sub>–ZrO<sub>2</sub>–SiC composition (appearance of peaks corresponding to ZrO<sub>2</sub>: angle  $2\theta = 22, 59$ )

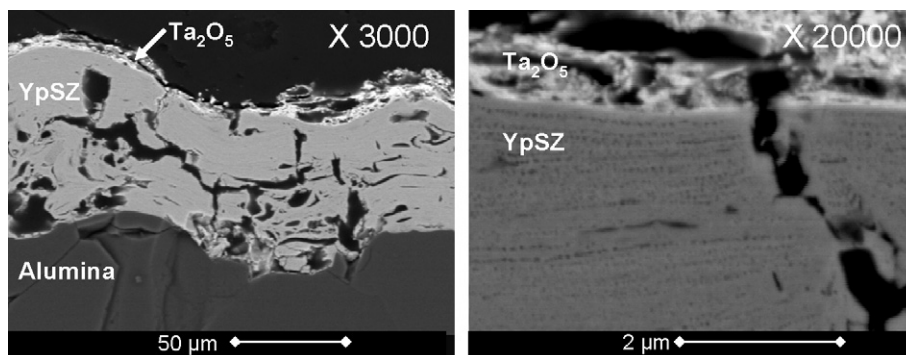


Fig. 5. Cross section of the YpSZ/Ta<sub>2</sub>O<sub>5</sub> stack observed by SEM (after the heat treatment at 1273 K for 4 h).

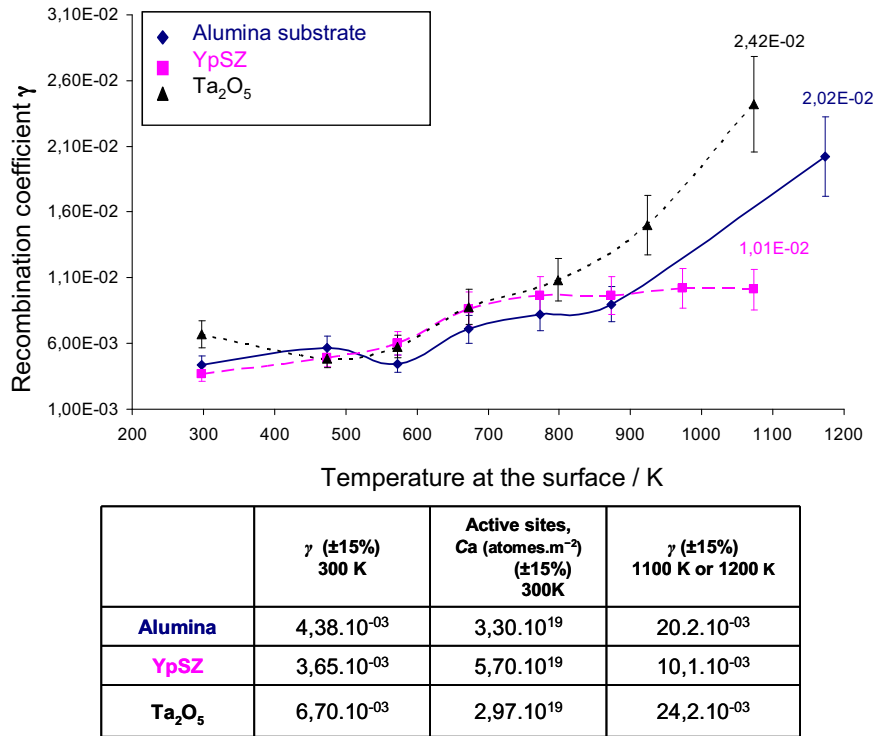


Fig. 6. Recombination coefficient  $\gamma$  and number of active sites estimated on alumina substrate, YpSZ and Ta<sub>2</sub>O<sub>5</sub> coatings.

but no silica layer was observed. This transformation involves the formation of boron oxides. B<sub>2</sub>O<sub>3</sub> can fill any cracks forming and thus prevent the diffusion of oxygen during atmospheric re-entry phase.

These results are in agreement with the SEM observation (Fig. 8). First of all, the thickness of the deposit is larger than one hundred microns and there is no problem of adhesion, even after exposure to an oxygen flux at 1273 K. The surface has a porous aspect, confirming the formation of ZrO<sub>2</sub>. A multi-layer system (SiO<sub>2</sub>, ZrO<sub>2</sub>, SiC + ZrO<sub>2</sub> layer) was not observed as expected.<sup>12,14</sup> This result can be explained by several factors. The first one is the nature of the deposit. A plasma spray test was performed on the silicon carbide sample, whereas samples used in the literature<sup>24</sup> were obtained by hot pressing of ZrB<sub>2</sub> and SiC powders. The second factor is the difference in the thermal

treatment in this work and other work. The maximum temperature and time of sample processing (2 h at 1273 K) are lower than those in the literature (temperature from 1473 K to 2473 K for treatment times between 30 and 60 min).

#### 4.2. Recombination of oxygen at the surface of ZrB<sub>2</sub>-ZrO<sub>2</sub>-SiC coatings

Due to the high exothermicity of the atomic oxygen recombination reaction during the space shuttle re-entry process, it is interesting to follow the evolution of gamma coefficient from 473 K to 1073 K. As shown in Fig. 9, the recombination coefficient increases with temperature and exhibits higher values than those measured on the other SiC samples (SiC + Chromium).<sup>25,26</sup>

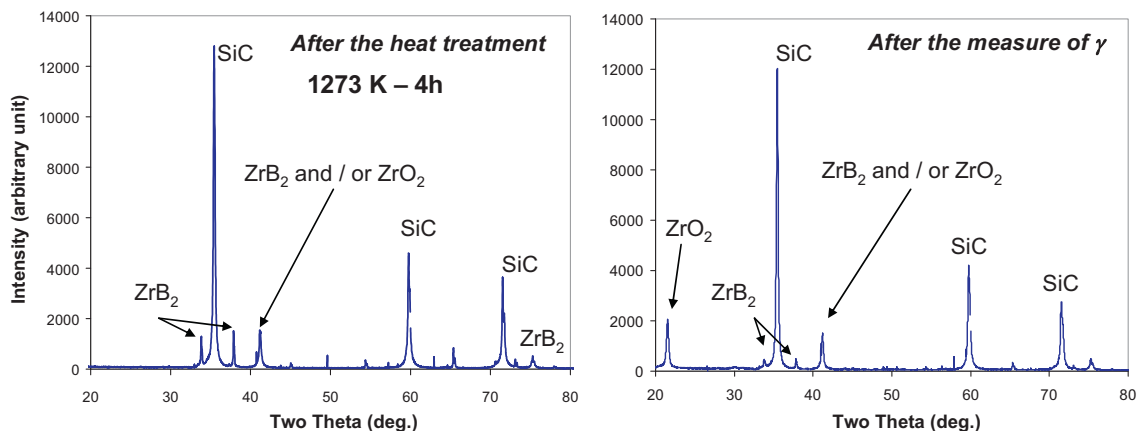


Fig. 7. XRD patterns of ZrB<sub>2</sub>-ZrO<sub>2</sub>-SiC performed after the heat treatment and the measure of  $\gamma$ .

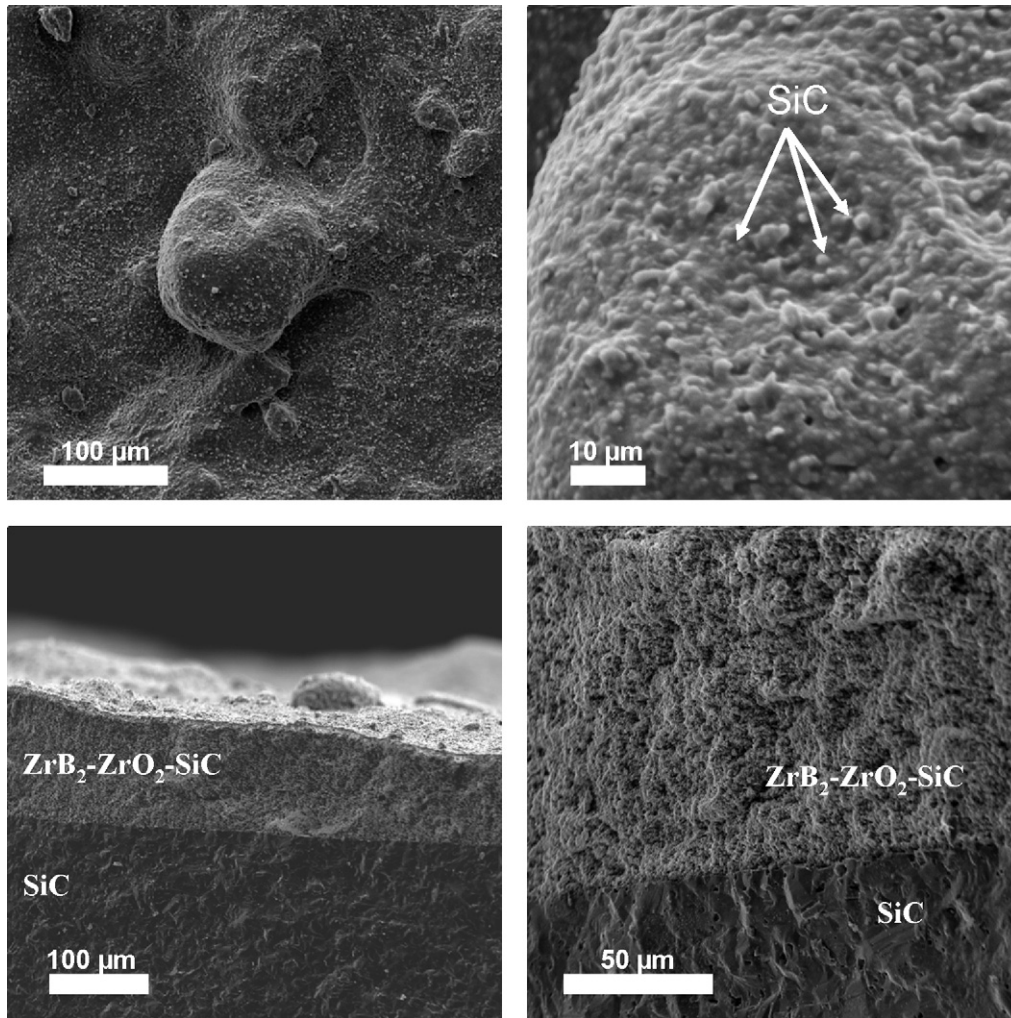


Fig. 8. Surface morphology and cross section of  $\text{ZrB}_2\text{-ZrO}_2\text{-SiC}$  observed by SEM after plasma exposure during the measurement of the recombination coefficient.

This behaviour can be explained by the fact that the nature of the surface changes during treatment. It has already been shown that the deposits of  $\text{ZrB}_2$  turned into  $\text{ZrO}_2$  and  $\text{B}_2\text{O}_3$ , thus greatly reducing the diffusion of oxygen. This change is found at 700 K which corresponds to the melting temperature of  $\text{B}_2\text{O}_3$  and the oxidation of  $\text{ZrB}_2$  into  $\text{ZrO}_2$ . At higher temperature, stabilization of the recombination coefficient is observed. At 1073 K, the

value of recombination is lower than the value of that for blank silicon carbide, close to that of the thermal barrier YpSZ but higher than that of Cr + SiC deposition. This is certainly due to a lack of silica on surface (less recombinant).

## 5. Conclusion

A low pressure plasma process has been developed for the deposition of complex ceramic oxides under low temperature conditions. The injection system of the reactor permits the injection of aqueous solutions and aqueous solution with solid suspensions. By using this technique, it was possible to obtain YpSZ and YpSZ/ $\text{Ta}_2\text{O}_5$  coatings for application as thermal barrier coatings (TBC) (growth rate:  $10 \mu\text{m h}^{-1}$ ). In particular, YpSZ exhibited micro and nano porosity which decreases the thermal diffusivity of the layer. The thermal diffusivity values obtained at high temperature are about one third of those obtained from plasma sprayed material. Measuring the recombination coefficient of both YpSZ and  $\text{Ta}_2\text{O}_5$  underlined the fact that the surface properties of the layers are quite different.  $\text{Ta}_2\text{O}_5$ , which is envisaged as a protective layer against atmo-

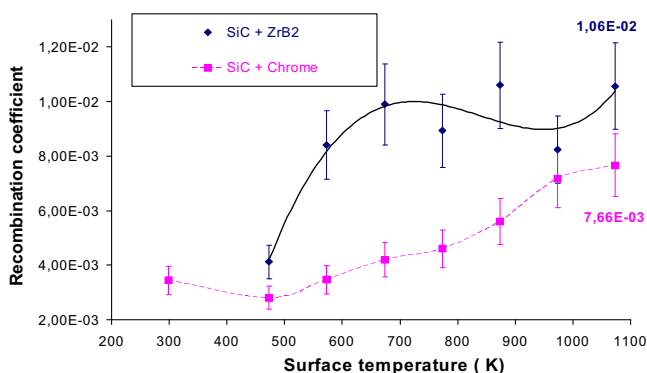


Fig. 9. Recombination coefficients  $\gamma$  versus surface temperature for  $\text{ZrB}_2\text{-ZrO}_2\text{-SiC}$  coatings.

spheric dust, could increase the diffusion of oxygen into the bulk of the coatings, which could lead to delamination of the TBC.

The deposition of complex ultra-high temperature composite material has also been achieved using the same process. A  $\text{ZrB}_2\text{-ZrO}_2\text{-SiC}$  coating up to  $100\ \mu\text{m}$  thick was deposited onto a SiC substrate ( $60\ \mu\text{m h}^{-1}$ ). No problem of adhesion was noted for the coating over a temperature range from 298 K to 1100 K. In comparison with the literature, no silica layer was observed despite the probable loss of silicon carbide. The formation of  $\text{B}_2\text{O}_3$  seems to be key for the prevention of the diffusion of oxygen during atmospheric re-entry phase. Moreover, treatments at higher temperatures seem necessary to validate the deposition technique (at least up to 2000 K) and more work on the diffusion of oxygen (using  $\text{O}^{18}$  in the plasma) in this type of layer would also be helpful.

## References

- Evans AG, Clarke DR, Levi CG. The influence of oxides on the performance of advanced gas turbines. *J Eur Ceram Soc* 2008;**28**:1405–19.
- Pature NP, Klemens PG. Low thermal conductivity in garnets. *J Am Ceram Soc* 1997;**80**:1018–20.
- Zhao H, Yu F, Bennett TD, Wadley HNG. Morphology and thermal conductivity of yttria-stabilized zirconia coatings. *Acta Mater* 2006;**54**:5195–207.
- Hwang C, Yu CH. Formation of nanostructured YSZ/Ni anode with pore channels by plasma spraying. *Surf Coat Technol* 2007;**201**:5954–9.
- Viazzi C, Bonino JP, Ansart F. Synthesis by sol–gel route and characterization of Yttria Stabilized Zirconia coatings for thermal barrier applications. *Surf Coat Technol* 2006;**201**:3889–93.
- Préaucht B, Drawin S. Properties of PECVD-deposited thermal barrier coatings. *Surf Coat Technol* 2001;**142–144**:835–42.
- Xie L, Ma X, Osturk A, Jordan EH, Pature NP, Cetegen BM, Xiao DT, Gell M. Processing parameter effects on solution precursor plasma spray process spray patterns. *Surf Coat Technol* 2004;**183**:51–61.
- Nagaraj B.A. et al. Thermal barrier coating protected by tantalum oxide and method for preparing the same. US Patent 6933066 B2, 2005, Assignee: General Electric Company. (Schenectady, NY, US).
- Krämer S, Faulhaber S, Chambers M, Clarke DR, Levi CG, Hutchinson JW, Evans AG. Mechanisms of cracking and delamination within thermal barrier systems in aero engines subject to Calcium–Magnesium–Alumino–Silicate (CMAS) penetration. *Mater Sci Eng* 2008;**A490**:26–35.
- Guo S-Q. Densification of  $\text{ZrB}_2$ -based composites and their mechanical and physical properties: a review. *J Eur Ceram Soc* 2009;**29**:995–1011.
- Chamberlain AL, Fahrenholtz W, Hilmas G, Ellerby D. Oxidation of  $\text{ZrB}_2\text{-SiC}$  ceramics under atmospheric and re-entry conditions. *Refract Appl Trans* 2005;**1(2)**:1–8.
- Han J, Hu P, Zhang X, Meng S, Han W. Oxidation-resistant  $\text{ZrB}_2\text{-SiC}$  composites at 2200 °C. *Compos Sci Technol* 2008;**68**:799–806.
- Peng F, Speyer RF. Oxidation resistance of fully dense  $\text{ZrB}_2$  with SiC, TaB<sub>2</sub>, and TaSi<sub>2</sub> additives. *J Am Ceram Soc* 2008;**91**:1489–94.
- Han WB, Hu P, Zhang XH, Han JC, Meng SH. High-temperature oxidation at 1900 °C of  $\text{ZrB}_{2-x}\text{SiC}$  ultrahigh-temperature ceramic composites. *J Am Ceram Soc* 2008;**91**:3328–34.
- Rousseau F, Awamat S, Nikravech M, Morvan D, Amouroux J. Deposit of dense YSZ electrolyte and porous NiO–YSZ anode for SOFC device by a low pressure plasma process. *Surf Coat Technol* 2007;**202**:1226–30.
- Rousseau F, Awamat S, Morvan D, Amouroux J, Mévrel R. Deposition of thick oxide layers from solutions in a low pressure plasma reactor. *Surf Coat Technol* 2007;**202**:714–8.
- Rousseau F, Awamat S, Morvan D, Prima F, Mévrel R. Yttria-stabilized zirconia thick coatings deposited from aqueous solution in a low pressure plasma reactor. *Surf Coat Technol* 2008;**203**:442–8.
- Mévrel R, Laizet J-C, Azzopardi A, Leclercq B, Poulain M, Lavigne O, Demange D. Thermal diffusivity and conductivity of  $\text{Zr}_{1-x}\text{Y}_x\text{O}_{2-x/2}$  ( $x=0, 0.084$  and  $0.179$ ) single crystals. *J Eur Ceram Soc* 2004;**24**:3081–9.
- Bertrand G, Bertrand P, Roy P, Rio C, Mévrel R. Low conductivity plasma sprayed thermal barrier coating using hollow pSZ spheres: correlation between thermophysical properties and microstructure. *Surf Coat Technol* 2007;**202**:1994–2001.
- Rousseau F, Nikravech M, Benabdelmoumene L, Guyon C, Morvan D, Amouroux J. Electrochemical studies on Sr doped LaMnO<sub>3</sub> and LaCoO<sub>3</sub> layers synthesised in a low-pressure plasma reactor equipped with a convergent nozzle. *J Appl Electrochem* 2007;**37(1)**:95–101.
- Guyon C, Cavadias S, Amouroux J. Heat and mass transfer phenomenon from an oxygen plasma to a semiconductor surface. *Surf Coat Technol* 2001;**142–144**:959–63.
- Guyon C, Cavadias S, Mabilie I, Moscova M, Amouroux J. Recombination of oxygen atomic excited states produced by non-equilibrium RF plasma on different semiconductor materials: catalytic phenomena and modelling. *Catal Today* 2004;**89**:159–67.
- Yan Y, Zhang H, Huang Z, Liu J, Jiang D. In situ synthesis of ultrafine  $\text{ZrB}_2\text{-SiC}$  composite powders and the pressureless sintering behaviors. *J Am Ceram Soc* 2008;**91**:1372–6.
- Fahrenholtz WG. Thermodynamic analysis of  $\text{ZrB}_2\text{-SiC}$  oxidation: formation of a SiC-depleted region. *J Am Ceram Soc* 2007;**90**:143–8.
- Da Rold G, Guyon C, Cavadias S, Amouroux J. Barriers of oxidation and ageing of space shuttle material. *Adv Mater Res* 2010;**89–91**:136–41.
- Da Rold G, Guyon C, Cavadias S, Amouroux J, Micheli V, Laidani N. Catalytic and ageing study of space shuttle material: regeneration of their original catalytic properties. *J High Temp Mater Proc* 2009;**13**:361–72.